The role of regulatory domain interactions in UNC-43 CaMKII localization and trafficking

Tohru Umemura, Paris Rapp and Christopher Rongo*

The Waksman Institute, Department of Genetics, Rutgers University, Piscataway, NJ 08854, USA

*Author for correspondence (e-mail: rongo@waksman.rutgers.edu)

Accepted 21 April 2005
Journal of Cell Science 118, 3327-3338 Published by The Company of Biologists 2005
doi:10.1242/jcs.02457

Summary

Calcium and calmodulin-dependent protein kinase II (CaMKII) plays a fundamental role in the synaptic plasticity events that underlie learning and memory. Regulation of CaMKII kinase activity occurs through an autoinhibitory mechanism in which a regulatory domain of the kinase occupies the catalytic site and calcium/calmodulin activates the kinase by binding to and displacing this regulatory domain. A single putative ortholog of CaMKII, encoded by *unc-43*, is present in the *Caenorhabditis elegans* nervous system. Here we examined UNC-43 subcellular localization in the neurons of intact animals and show that UNC-43 is localized to clusters in ventral cord neurites, as well as to an unlocalized pool within these neurites. A mutation that mimics autophosphorylation within the regulatory domain results in an increase in the levels of UNC-43 in the unlocalized neurite pool. Multiple residues of CaMKII facilitate the interaction between the catalytic domain and the regulatory domain, thereby keeping the kinase inactive. Whereas most mutations in these residues result in an increased neurite pool of UNC-43, we have identified two residues that result in the opposite effect when mutated: a decreased neurite pool of UNC-43. The activity of UNC-2, a voltage-dependent calcium channel, is also required for UNC-43 to accumulate in the neurites, suggesting that neural activity regulates the localization of UNC-43. Our results suggest that the activation of UNC-43 by calcium/calmodulin displaces the autoinhibitory domain, thereby exposing key residues of the catalytic domain that allow for protein translocation to the neurites.

Key words: CaMKII, Trafficking, *Caenorhabditis elegans*, UNC-43

Introduction

An important objective in neuroscience is to determine how molecular and cell biological changes in the nervous system play a role in acquiring and storing memories. One of the key regulatory molecules involved in memory acquisition, consolidation and retrieval is the calcium and calmodulin-dependent kinase type II (CaMKII), which was originally identified as an abundant brain protein found at the postsynaptic density (reviewed by Hudmon and Schulman, 2002; Rongo, 2002). Pharmacological blockers of CaMKII or mutations in the mouse alpha subunit of CaMKII reduce long term potentiation (LTP) in the hippocampus (Hinds et al., 1998; Ito et al., 1991; Lisman and Goldring, 1988; Malenka et al., 1989; Malinow et al., 1989; Silva et al., 1992b). Moreover, knockout mice show impaired spatial learning, suggesting that CaMKII regulates the molecular events underlying synaptic plasticity (Silva et al., 1992a). One of the mechanisms by which CaMKII regulates plasticity is by regulating the subcellular localization of AMPA-type glutamate receptors (AMPARs) in response to neural activity and subsequent calcium influx (Hayashi et al., 2000; Rongo and Kaplan, 1999).

CaMKII activity is regulated by calcium through its interaction with calmodulin (Meador et al., 1993). The kinase comprises multiple subunits that associate to form a holoenzyme (Brocke et al., 1999; Gaertner et al., 2004; Hoelz et al., 2003). Each subunit consists of a bi-lobed catalytic domain, which includes an N-terminal lobe containing the catalytic core and a C-terminal lobe containing multiple α helices and an autoinhibitory domain. In the absence of calcium signaling, CaMKII is inactive because the autoinhibitory domain binds to the catalytic domain along two hydrophobic pockets, thereby preventing access to substrate (Yang and Schulman, 1999). In the presence of calcium signaling, calcium-bound calmodulin binds to specific residues within the autoinhibitory domain, causing its displacement and exposing a critical threonine, T286, on the autoinhibitory domain. The T286 residue is phosphorylated by adjacent subunits in the holoenzyme upon displacement by calcium/calmodulin (Hanson et al., 1994; Mukherji et al., 1994; Mukherji and Soderling, 1994; Rich and Schulman, 1998). Once phosphorylated at T286, the autoinhibitory domain can no longer interact with the catalytic domain, thus allowing the catalytic domain to access and thus phosphorylate substrates. Threonine to aspartate (T286D) substitutions can mimic autophosphorylation of CaMKII by introducing charge on the autoinhibitory domain, resulting in the displacement of the domain and calcium-independent activity (Fong et al., 1989; Waldmann et al., 1990). Interestingly, the conformational changes induced by autophosphorylation can allow the catalytic domain to interact with other proteins that are similar in sequence to the autoinhibitory domain. For example, sequences within the NR2B NMDA receptor subunit can bind to CaMKII by mimicking the autoinhibitory domain, resulting in a CaMKII that is locked into an active state (Bayer et al., 2001).

CaMKII is found in dendrites, where it colocalizes at or near the postsynaptic densities (PSDs) of synapses, as well as at non-synaptic clusters (Ouimet et al., 1984; Petersen et al., 2003; Strack et al., 1997; Tao-Cheng et al., 2002). Studies using both dissociated neurons and hippocampal slices indicate that CaMKII localization is regulated in response to activity and autophosphorylation (Leonard et al., 1999; Ouyang et al., 1997; Shen and Meyer, 1999; Shen et al., 2000; Strack et al., 1997). However, CaMKII localization is complicated by the presence of multiple isoforms, which can be targeted to distinct sites of subcellular localization (Gaertner et al., 2004; Shen and Meyer, 1999). Holoenzymes can consist of a mixture of different subunit types, which can alter CaMKII localization. An additional complication is that ischemia can affect the localization of CaMKII, resulting in clustering of the kinase during the production of hippocampal slices and dissociated hippocampal neurons (Tao-Cheng et al., 2002).

An alternative approach to understanding CaMKII function and subcellular localization is to use the genetics and simple nervous system of the nematode *C. elegans*, as the clear cuticle of *C. elegans* affords the opportunity to observe protein trafficking and localization to synapses in the intact central nervous system of a living animal. *C. elegans* possesses only a single isoform of CaMKII, called *unc-43*, which is alternatively spliced into multiple transcripts (Reiner et al., 1999). Null mutants for *unc-43* show increased neuromuscular activity in locomotory, egg-laying and defecation circuits, whereas gain-of-function mutants show decreased activity for these same circuits. However, it is unclear which of the specific *unc-43* splice forms conducts each of these different functions. Moreover, the specific neuronal circuits in which *unc-43* conducts each of these functions is currently unknown.

UNC-43 has also been shown to regulate the synaptic trafficking of GLR-1, an AMPA-type glutamate receptor, in a specific circuit of about a dozen *C. elegans* interneurons (Rongo and Kaplan, 1999). Although the exact isoforms that conduct this function are not known, the UNC-43G isoform (WormBase nomenclature) in particular can rescue the *unc-43* mutant phenotype with respect to GLR-1 localization (Chen et al., 2005; Rongo and Kaplan, 1999). These GLR-1-expressing interneurons project single unbranched processes with both axonal and dendritic character (henceforth referred to as 'neurites' for simplicity) into the nerve ring and ventral cord fascicles, where they receive input from glutamatergic sensory neurons and output to motorneurons through en passant synapses (Chalfie et al., 1985; Hart et al., 1995; Maricq et al., 1995; White et al., 1986). A chimeric GLR-1::GFP protein is localized to sensory-interneuron and interneuron-interneuron synapses; however, in *unc-43* null mutants, GLR-1::GFP accumulates in perinuclear puncta in the cell bodies of the interneurons. Cell autonomous expression of the UNC-43G isoform in these neurons is sufficient to rescue these defects in GLR-1 localization. However, the relevant targets of UNC-43 in these neurons are unknown.

Here we show that a GFP-tagged chimeric UNC-43 protein is found to be localized both in clusters along the ventral cord neurites, and in a diffuse unlocalized pool within neurites. Mutations known to mimic autophosphorylation of the kinase result in an increase in the abundance of the kinase in neurites, particularly in the unlocalized neurite pool. We find that two key residues of the catalytic domain that stabilize its interaction with the autoinhibitory domain are also required for the kinase to accumulate in neurites and for its function with respect to GLR-1 localization. Our results suggest that although kinase activity itself does not regulate UNC-43 localization, it nevertheless changes the conformation of the kinase, exposing critical residues in the catalytic core required for it to accumulate in neurites.

Materials and Methods

Genetics and strains

Standard methods were used to handle and maintain *C. elegans* (Wood, 1988). We used the following strains: N2, *unc-43(n1186)*, *nuIs25[glr-1::gfp]*, *nuIs68[unc-43::gfp]*, *odIs1[snb-1::gfp]* and *unc-2(e55)*.

Transgenes and germline transformation

Transgenic strains were isolated by microinjecting various plasmids (typically at 50 ng/μl) using either *lin-15(+)* (a gift from J. Mendel, Caltech, Pasadena, CA) or *rol-6dm* (a gift from C. Mello, University of Massachusetts Medical School, Worcester, MA) as a marker. The resulting transformants were followed as extrachromosomal arrays. The *unc-43::gfp* transgene was generated by subcloning sequences encoding GFP in-frame at the N-terminus of *unc-43* cDNA. Sequences for the resulting chimeric protein were placed into the *glr-1* promoter vector pV6 (a gift from Villu Maricq, University of Utah, Salt Lake City, UT). Truncated versions of *unc-43::gfp* were generated by using a corresponding set of primers to make a PCR product of the partial *unc-43* cDNA, which was then used to replace sequences in-frame, encoding the full-length *unc-43* cDNA in the *unc-43::gfp* transgene. Mutated versions of *unc-43::gfp* were generated by using oligonucleotide-mediated mutagenesis to introduce amino acid substitutions into an *unc-43* cDNA, which was then used to replace the *unc-43* cDNA in the *unc-43::gfp* transgene. The $P_{glr\text{-}1}$*::unc-43* transgene was generated by subcloning sequences encoding *unc-43* cDNA into the *glr-1* promoter vector pV6. Mutated versions of $P_{glr\text{-}1}$*::unc-43* were generated using oligonucleotide-mediated mutagenesis as above. All described constructs were confirmed by DNA sequencing.

S2 cell expression

Plasmids for expression in S2 insect cell lines were generated by subcloning sequences encoding the *unc-43* cDNA into pMT/V5, an expression vector containing the *Drosophila* metallothionein promoter and a V5 epitope (Invitrogen). Mutated *unc-43* cDNA sequences were similarly placed into pMT/V5. Rat CaMKII (a gift from Mary Kennedy, Caltech, Pasadena, CA) and CaMKII(T286D) (a gift from Howard Schulman, Stanford University School of Medicine, Stanford, CA) cDNA sequences were also introduced into pMT/V5. Expression constructs were transfected into growing S2 cells and induced by the addition of copper. Cells were harvested 24 hours after transfection. Cells were lysed in lysis buffer [50 mM PIPES, pH 7.0, 1 mM EGTA, 10% glycerol, 2 mM DTT, 1 mM PMSF, antiprotease cocktail (Roche)] using a dounce homogeniser. The lysates were then centrifuged at 16,000 ***g*** for 5 minutes, and the supernatant was collected for analysis. The quantity of wild-type and mutant UNC-43 and CaMKII kinases present in the lysates was determined by immunoblotting using anti-V5 antibodies (Invitrogen). Immunoblot analysis demonstrated that the kinase and its mutant forms were at or near full length.

Kinase assays

Kinase activity was measured using the CaMKII-specific substrate AC-2 (KKALRRQETVDAL). Kinase activity was measured at 30°C

in reactions containing 50 mM PIPES, pH 7.0, 10 mM $MgCl_2$, 0.1 mg/ml BSA, 0.1 mM $CaCl_2$, 50 μM ATP containing [γ-^{32}P]ATP, 1 μM calmodulin and 20 mM AC-2. The average kinase activity of untransfected S2 cell lysates was subtracted prior to plotting the activities shown in Fig. 4. The calcium/calmodulin-independent activity was determined in the absence of calcium and calmodulin, and with the addition of 5 mM EGTA.

Fluorescent microscopy

GFP- and RFP-tagged fluorescent proteins were visualized in nematodes by mounting larvae on 2% agarose pads with 10 mM levamisole at room temperature. Fluorescent images were observed using a Zeiss Axioplan II and 100× 1.4 NA PlanApo objective and imaged with an ORCA CCD camera (Hamamatsu) using ImagePro v4.1 and VayTek v6.2 software. Exposure times were chosen to fill the 12-bit dynamic range without saturation. Animals were optically sectioned (0.4 μm) and out-of-focus light was removed with a constrained iterative deconvolution algorithm (VayTek).

To quantify the fluorescence levels of GFP-tagged proteins, images of nematodes were captured by CCD as above, using a constant gain and exposure time (filled the 12-bit dynamic range) for all samples. A fluorescent standard (Labsphere) showed less than 1% drift in signal throughout the imaging session. Images were corrected for coverslip fluorescence by subtracting a background image. Pixel intensity was measured for each animal by quantifying an area of interest that collected the fluorescent ventral nerve cord for each sample. The peak amplitude of clusters (localized signal) was calculated for each two-dimensional projection as the fractional increase over the diffuse background of ventral cord fluorescence (unlocalized baseline). Cluster outlines were automatically calculated for fluorescent signals that were two standard deviations above the unlocalized baseline for wild-type UNC-43::GFP using a macro written for ImagePro. Cluster number was calculated by counting the average number of clusters per 10 μm of neurite length. The amount of unlocalized UNC-43 was calculated by measuring the average fluorescence of the diffuse background of the ventral cord. Statistical comparisons were performed using Prism 4.0 (GraphPad). Images of nematodes expressing fluorescent proteins from extrachromosomal arrays were only captured if the array was present in all the GLR-1-expressing cells previously reported.

Real-time PCR

An integrated array (*nuIs68*) of the *unc-43::gfp* transgene was generated by UV-mediated integration (Rongo and Kaplan, 1999). The *nuIs68* integrant was backcrossed four times and was inherited in a mendelian fashion. RNA was prepared from worms carrying two copies of the *nuIs68* array using strains homozygous for the array. RNA was prepared from worms carrying one copy of the *nuIs68* array by mating homozygous *nuIs68* males into wild-type N2 hermaphrodites, then selecting fluorescent cross progeny. Total RNA from mixed stage worms of both genotypes was prepared using Trizol (Invitrogen). First-strand reverse transcription was performed with 800 ng total RNA using iScript (Biorad) as per the manufacturer's instructions. Real-time PCR reactions were performed with 5 ng of template using iQ SYBR Green (Biorad) and a Rotorgene 3000 as per the manufacturer's instructions. Primer sets detected either GFP or *dlg-1*, a control transcript of an adherens junction protein (Firestein and Rongo, 2001). No product was detected for the GFP primer sets in reversed-transcribed RNA from N2 nematodes. No products were detected for either primer set for RNA that was processed in the absence of reverse-transcription. Standard curves of reversed-transcribed RNA from homozygous *nuIs68* were generated and analyzed in triplicate by dilution over three orders of magnitude. Calibration curves were linear over this complete range (R^2=0.990 for GFP primers, R^2=0.992 for *dlg-1* primers). Concentrations were derived by comparing *Ct* (threshold cycle) values of samples (performed 4-8 times/genotype) to the standard curves. For each genotype, mean GFP expression measurements were normalized to those for *dlg-1*.

Rescue of GLR-1 localization

To determine whether the mutant versions of UNC-43 could rescue the GLR-1 localization defects of an *unc-43* null mutant, we generated the $P_{glr\text{-}1}$*::unc-43* transgenes either with or without the *unc-43* mutations. Individual transgenes were co-injected with *rol-6dm* as a marker into *nuIs25[glr-1::gfp]; unc-43* mutants, and transgenic lines were obtained. Rescue was scored by measuring the cell body levels of GLR-1::GFP that accumulated, using the same methodology used to measure UNC-43::GFP cell body levels described above.

Results

UNC-43 translocation in neurons

We previously observed UNC-43 subcellular localization in neurons by generating a chimeric protein in which UNC-43 sequences are fused to GFP sequences at the GFP C-terminus (Rongo and Kaplan, 1999). The resulting transgene, which contains the *glr-1* promoter, was introduced into nematodes where it expressed UNC-43::GFP specifically in the small number of neurons that also express GLR-1 AMPARs. To further explore UNC-43 localization, we generated an *unc-43::cfp* transgenic strain using the same approach as for *unc-43::gfp*. To avoid assaying holoenzymes of mixed composition (e.g. mixes of wild-type and mutant subunits, or GFP-tagged and untagged subunits), we introduced the transgene (and subsequent transgenes) into *unc-43(n1186)* null mutants that lack the endogenous subunit. The resulting UNC-43::CFP protein was detected in neuron cell bodies (Fig. 1A) and out at neurites (Fig. 1B), where it formed clusters along the ventral nerve cord. We previously showed that the *unc-43::gfp* transgene is functional as it rescues an *unc-43* null mutant phenotype for the locomotion defects when expressed in most neurons using a heat-shock promoter (Rongo and Kaplan, 1999).

UNC-43 regulates the translocation of GLR-1 AMPARs to synaptic clusters in the fascicle of neurites found in the ventral nerve cord (Rongo and Kaplan, 1999). To determine if UNC-43 colocalizes with GLR-1, we introduced the *unc-43::cfp* transgene into nematodes expressing *glr-1::yfp*, a transgene containing a full-length GLR-1 tagged with YFP (Rongo et al., 1998). GLR-1 colocalizes with Golgi-resident proteins at punctate structures within the cell body (Glodowski et al., 2005; Shim et al., 2004) (Fig. 1C and data not shown). We detected UNC-43::CFP at punctate structures in the cell body (Fig. 1A), which colocalized with GLR-1::YFP puncta (Fig. 1E). We also found that 46±4% (mean±s.e.m. of 42 animals) of UNC-43::CFP puncta colocalized with GLR-1::YFP puncta in neurites (Fig. 1F). There was also an unclustered, non-synaptic pool of UNC-43::CFP found throughout the ventral cord neurites. We obtained similar results through double-label analysis of UNC-43::GFP and GLR-1::RFP, a version of GLR-1 containing mRFP instead of YFP (Glodowski et al., 2005).

We wanted to test whether the activation of UNC-43 could regulate its translocation within neurons. We engineered the T286D mutation, which mimics autophosphorylation and results in calcium-independent kinase activity, into our UNC-

43::GFP transgene (Fong et al., 1989; Waldmann et al., 1990). Like wild-type UNC-43::GFP (Fig. 1G), we found that UNC-43(T286D)::GFP could be detected in the neuron cell body and out at the neurites (Fig. 1H and data not shown). Interestingly, we observed higher levels of fluorescence in the ventral cord neurites for UNC-43(T286D)::GFP than for wild-type UNC-43::GFP (Fig. 1M). By contrast, we observed fewer clusters of UNC-43(T286D)::GFP in the ventral cord than wild-type UNC-43::GFP (Fig. 1O).

One explanation for the different levels found in the ventral cord could be the difference in expression levels for UNC-43::GFP and UNC-43(T286D)::GFP. As our UNC-43::GFP transgenes only generate protein in a small number of neurons (the GLR-1-expressing interneurons), we have been unable to detect the protein by western analysis (data not shown). As an alternative, we measured the levels of different GFP-tagged chimeric proteins by quantitative epifluorescence. To calibrate our measurements, we measured the relative levels of UNC-43::GFP from nematodes that carried either one or two copies of a genome-integrated UNC-43::GFP transgenic array. We confirmed that the transcript levels of these strains reflected the array copy number by measuring *unc-43::gfp* mRNA using real-time PCR (Fig. 1I). As expected, we detected a twofold difference in *unc-43::gfp* mRNA (Fig. 1I), and in fluorescence levels both in the cell body (Fig. 1J) and in the neurites (Fig. 1K). We next measured UNC-43::GFP and UNC-43(T286D)::GFP cell body levels and detected no significant difference in expression (Fig. 1L).

To determine how the T286D mutation affects UNC-43::GFP translocation, we next examined and measured the levels of wild-type UNC-43::GFP and UNC-43(T286D)::GFP in neurites. We measured their amounts in the ventral cord by

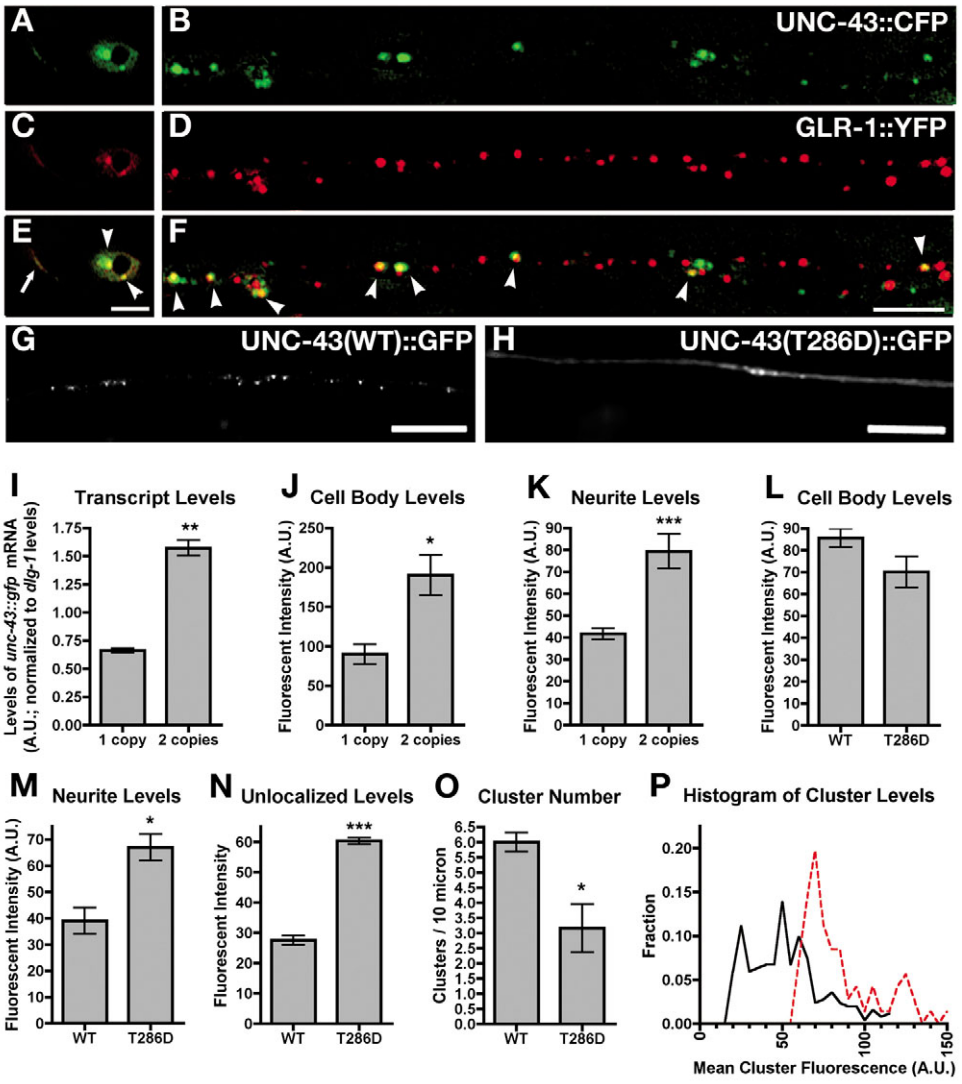

Fig. 1. The *Caenorhabditis elegans* CaMKII ortholog UNC-43 is localized to neurites. (A,B) UNC-43::CFP and (C,D) GLR-1::YFP can be detected in perinuclear structures in neuronal cell bodies (A,C) and clusters within the neurites of the ventral nerve cord (B,D). Merged images for A-D indicate that UNC-43 and GLR-1 colocalize (arrowheads) at perinuclear structures (E), and at a fraction of neurite clusters (F). Arrow in E indicates a unipolar neurite, partially out of the focal plane, extending from the cell body. Gray-scale images of UNC-43::GFP (G) and UNC-43(T286D)::GFP (H) indicate that the T286D change increases the amount of UNC-43 found diffusely distributed throughout the neurites. (I) Real-time PCR measurements of *unc-43::gfp* mRNA for nematodes expressing either one or two copies of an *unc-43::gfp* integrated transgene. Values are normalized to real-time PCR measurements of a *dlg-1* control transcript. A significant difference in the level of expression was observed, $^{**}P<0.001$ using Student's *t*-test ($n=4$), between the two groups. Fluorescence quantification measuring the mean fluorescent intensity values for neuron cell bodies (J) or neurites expressing either one copy or two copies of an *unc-43::gfp* transgene integrated into the genome (K). Fluorescence quantification measuring the mean fluorescent intensity values for neuron cell bodies (L), neurites including clustered and unlocalized fluorescence (M) and unlocalized fluorescence alone (N) (i.e., diffuse fluorescence defined by a threshold within two standard deviation values of the mean outside of the clustered signal) for nematodes expressing either UNC-43::GFP or UNC-43(T286D)::GFP. (O) The number of clusters (clusters defined as above a threshold of two standard deviation values of the mean outside of the clustered signal) per 10 μm length of neurite. (P) Frequency distribution plots of the mean fluorescence values of UNC-43::GFP clusters (straight black line) or UNC-43(T286D)::GFP clusters (dashed red line). A.U., arbitrary fluorescence units. Error bars indicate s.e.m. Significant differences $^{*}P<0.01$, $^{***}P<0.0001$ were observed using the Student's *t*-test between the indicated test groups and the WT or single copy control group. n=10-25 animals per genotype. Bar 5 μm (A-F); 10 μm (G-H).

summing both the unlocalized pool of fluorescence distributed throughout the neurites and the fluorescence localized into clusters (defined as peaks of fluorescence that rise above a threshold two standard deviations above the mean unlocalized baseline measurements; Fig. 1M). We also measured the mean level of the unlocalized pool of fluorescence in the cord alone, which excludes the signal in fluorescent clusters (Fig. 1N) and found that UNC-43(T286D)::GFP accumulated within the unlocalized pool at roughly twice the level of UNC-43::GFP. As this difference cannot be explained by differences in expression level, our results suggest that the T286D mutation results in an increased accumulation of UNC-43::GFP throughout the ventral cord neurites, the bulk of which is found in an unlocalized pool within these neurites.

We noticed that there was a twofold reduction in the number of UNC-43(T286D)::GFP clusters relative to UNC-43::GFP clusters (Fig. 1O), and we reasoned that the dimmest population of UNC-43(T286D)::GFP clusters might not be detected above the now higher baseline of unlocalized UNC-43(T286D)::GFP (i.e. ~59 A.U. compared to ~27 A.U. for UNC43::GFP; Fig. 1N). To examine this possibility, we plotted frequency distributions (Fig. 1P) for the mean fluorescence levels of clusters for UNC-43::GFP (black solid line) and UNC-43(T286D)::GFP (red dotted line). Consistent with our hypothesis, about 50% of wild-type UNC-43::GFP clusters fall below the baseline level (~59 A.U.) found for UNC-43(T286D)::GFP (Fig. 1P). If UNC-43(T286D)::GFP had similar cluster fluorescent intensities as wild-type UNC-43::GFP, then we would expect to see about half as many clusters as wild-type UNC-43::GFP, which is consistent with our observations (Fig. 1O). Taken together, our results suggest that by mimicking activation of UNC-43 by the T286D mutation, we can increase the amount of UNC-43 present in the unlocalized pool in neurites.

Identification of inhibitory residues critical for UNC-43 autoregulation

As a first step to connecting the activity-dependent autoregulation of UNC-43 to its mechanism of subcellular localization, we examined the critical amino acids involved in keeping the kinase in its basal state. The regulation of CaMKII kinase activity occurs through an autoinhibitory domain that blocks the ability of the catalytic site to bind to substrate (Yang and Schulman, 1999) (Fig. 2A,B). A number of charged residues in the CaMKII autoinhibitory domain are thought to help mediate its interaction with the catalytic domain. For example, R283 in the autoinhibitory domain is thought to form an electrostatic interaction with D238 in the catalytic domain (Goldberg et al., 1996; Yang and Schulman, 1999). Another charged residue in the autoinhibitory domain, H282, is thought to form an electrostatic interaction with K148 in the catalytic domain (Goldberg et al., 1996; Yang and Schulman, 1999). Two hydrophobic regions on the catalytic domain of CaMKII are thought to help mediate its interaction with the autoinhibitory domain, and are conserved in UNC-43 (Goldberg et al., 1996; Yang and Schulman, 1999) (Fig. 2A). These residues are all conserved in the autoinhibitory domain of UNC-43 (Fig. 2A).

Interactions between the catalytic and autoinhibitory domains regulate translocation

The T286D mutation, which constitutively activates the kinase, can mobilize UNC-43 to the neurites. One explanation could be that kinase activation per se results in the increased translocation of UNC-43 to the neurites, perhaps by allowing the protein to bind to a mobile substrate. Alternatively, kinase activation might change the conformation of UNC-43, thereby allowing an unknown transport factor to interact with the protein and translocate it to the neurites. For

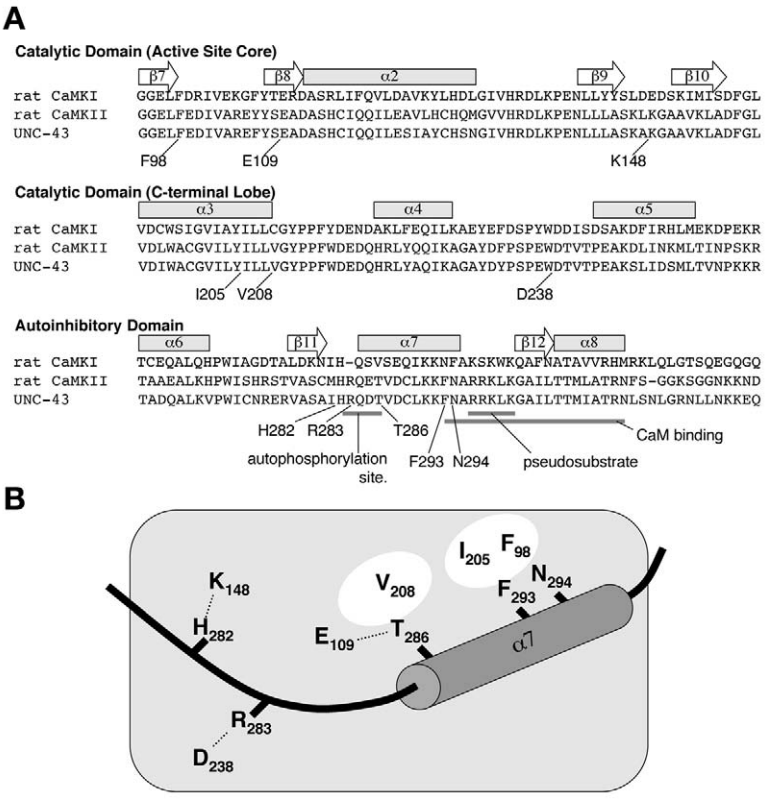

Fig. 2. Amino acid interactions between the catalytic domain and the autoinhibitory domain regulate UNC-43 calcium-independent activity. (A) Amino acid sequence alignments between rat CaMKI, rat CaMKII and UNC-43 for three key domains: the active site core of the catalytic domain, the C-terminal lobe of the catalytic domain and the autoinhibitory domain. Residues changed in this study are indicated using rat CaMKII numbering. The CaMKII autophosphorylation site, calmodulin (CaM) binding site, and the pseudosubstrate domain are delimited by gray lines below the sequence. The secondary structure elements described for the CaMKI crystal structure are indicated above the lines, using gray boxes for α helices and white arrows for β strands (Goldberg et al., 1996). (B) A schematic model for CaMKII and UNC-43 regulatory amino acid interactions between the catalytic domain (the gray box) and the autoinhibitory domain (the black line and gray cylinder). Electrostatic interactions between amino acid side chains are indicated by a dotted line. Hydrophobic pockets created within the catalytic domain are indicated by the white ovals.

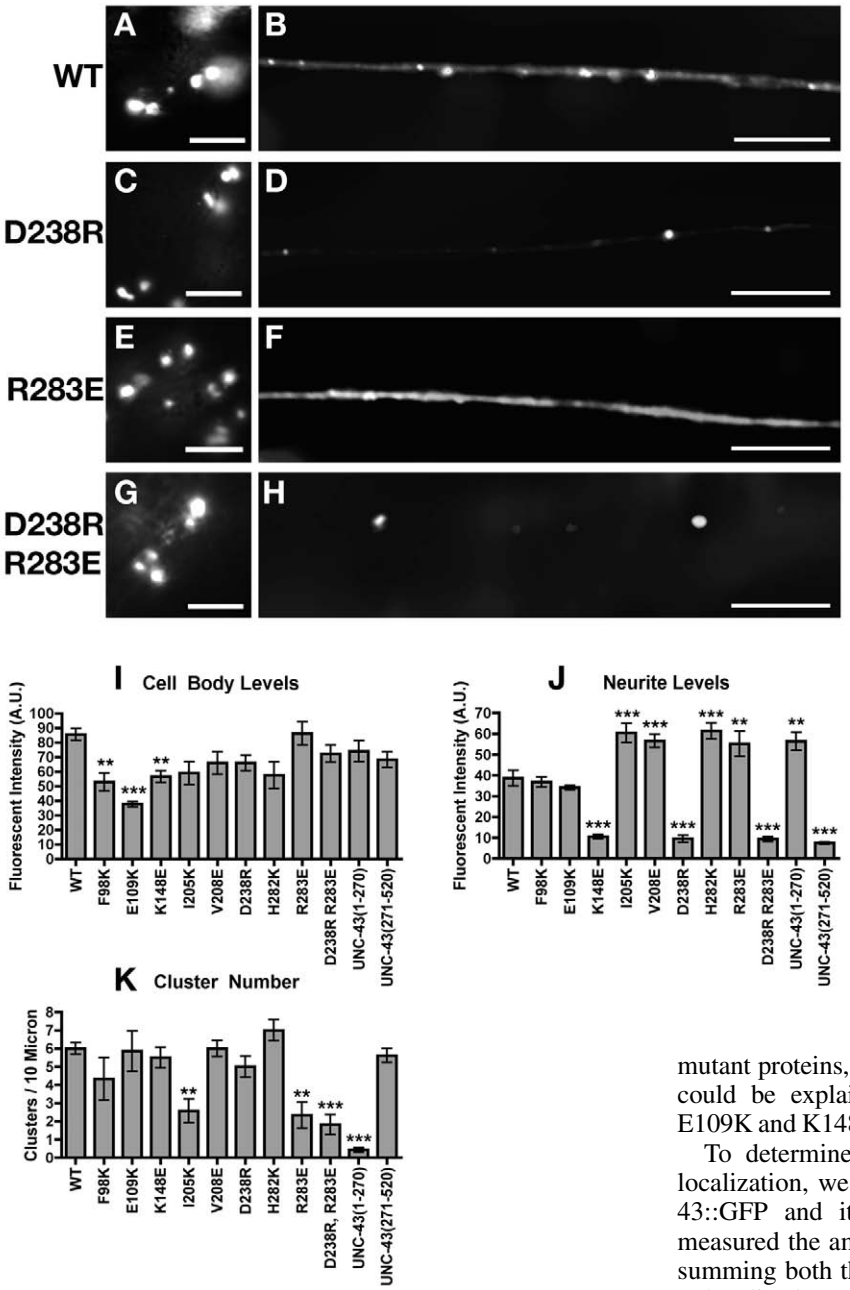

Fig. 3. Autoinhibitory domain interactions regulate UNC-43 abundance in the neurites. Cell bodies and neurites expressing (A,B) wild-type UNC-43::GFP, (C,D) UNC-43(D238R)::GFP, (E,F) UNC-43(R283E)::GFP and (G,H) UNC-43(D238R, R283E)::GFP. Mutations in D238 result in the failure of UNC-43 to accumulate throughout the unlocalized neurite pool (D), whereas mutations in R283 (F) result in the overabundance of UNC-43 in this pool. The phenotype of the two mutations combined (H) is similar to that of D238R alone (D). (I,J) Fluorescence quantification measuring the mean fluorescent intensity values for neuron cell bodies (I) and neurites (J) expressing the indicated UNC-43::GFP construct. (K) The number of clusters (clusters defined as above a threshold of two standard deviation values of the mean outside of the clustered signal) per 10 μm length of neurite. WT indicates the wild-type UNC-43 protein, and an amino acid substitution number identifies each mutant form of UNC-43 tested. The catalytic domain, identified as UNC-43(1-270), and the subunit association domain, identified as UNC-43(271-520) were also tested. A.U., arbitrary units. Error bars indicate s.e.m. Significant differences were observed $^{**}P<0.01$, $^{***}P<0.001$ compared to levels in the WT groups using one-way ANOVA followed by Dunnett's *t*-test comparisons. n=10-25 for each genotype. Bar, 5 μm.

example, the NR2B subunit of the NMDAR is thought to interact with the CaMKII catalytic domain in a similar fashion as the autoinhibitory domain (Bayer et al., 2001). To explore these possibilities, we introduced the previously described mutations into UNC-43::GFP to test whether all or only a subset of mutations that result in calcium-independent activity also result in increased UNC-43::GFP translocation.

Like wild-type UNC-43::GFP (Fig. 3A,B), we found that our mutant UNC-43::GFP proteins could be detected in the neuron cell body and out at the neurites (Fig. 3C-H, and data not shown) when introduced into nematodes. We measured the cellular levels of UNC-43::GFP and its mutant forms, and for most mutants we found no statistically-significant difference when compared to wild-type UNC-43::GFP (Fig. 3I). Three mutant proteins, however, showed a lower cellular level, which could be explained if the corresponding mutations (F98K, E109K and K148E) made the UNC-43::GFP protein less stable.

To determine how the mutations affected UNC-43::GFP localization, we next measured the levels of wild-type UNC-43::GFP and its mutant forms in neurites (Fig. 3J). We measured the amount of UNC-43::GFP in the ventral cord by summing both the fluorescence localized into clusters and the unlocalized pool of fluorescence distributed throughout the core of the neurites. Surprisingly, although the mutations result in increased calcium-independent CaMKII kinase activity (Yang and Schulman, 1999), only a subset altered UNC-43::GFP localization (and in very disparate ways). Mutations in F98K, which reduce the affinity of CaMKII for substrate (Yang and Schulman, 1999), show no effect on UNC-43::GFP localization. Mutations in the two hydrophobic regions of the catalytic domain (I205K and V208E) that stabilize its interaction with the autoinhibitory domain (Yang and Schulman, 1999) behave in a similar manner to T286D with respect to localization: increased levels of unlocalized UNC-43::GFP are found in neurites (Fig. 3J). All three of these interactions occur through the α7 helix of the autoinhibitory domain. The autoinhibitory domain also contains a loop of residues N-terminal to the α7 helix (Fig. 2B). Mutations in this loop (H282K and R283E) result in increased calcium-

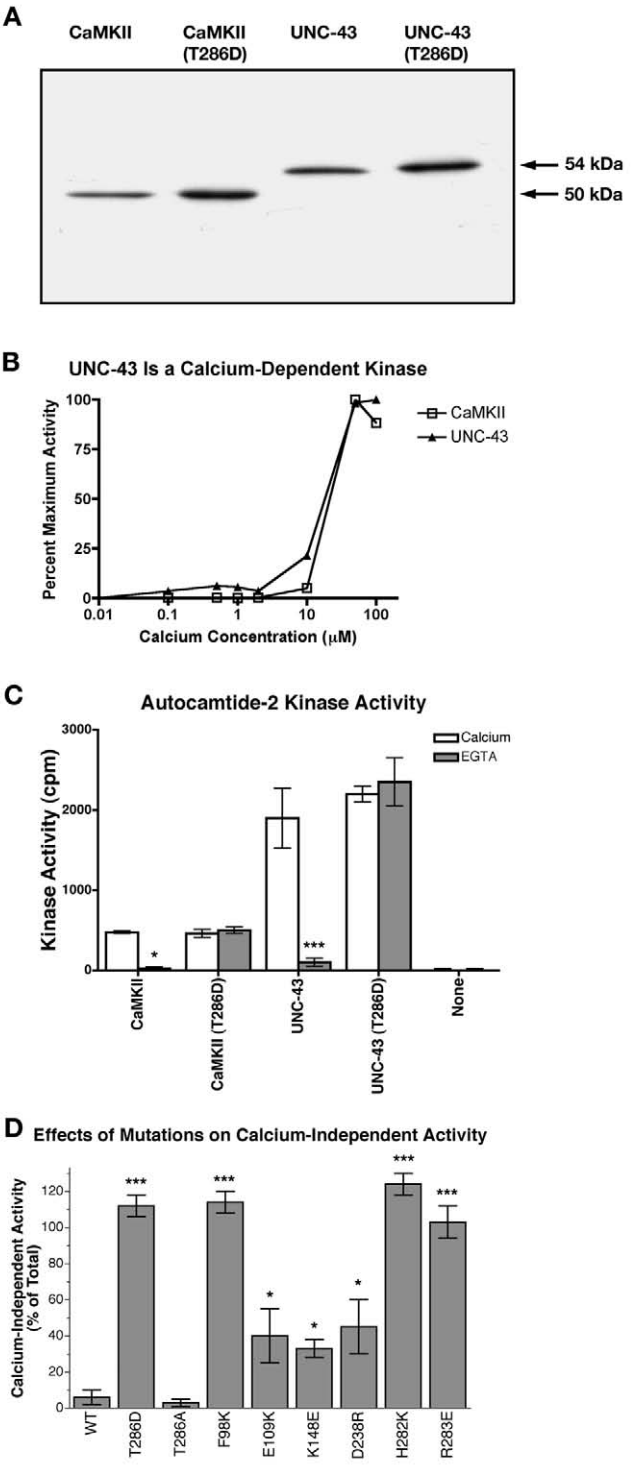

Fig. 4. UNC-43 calcium-dependent kinase activity. (A) S2 cells were transfected with the indicated cDNAs, then lysed and immunoblotted using anti-V5 antibodies to detect the recombinant proteins. (B) S2 cell lysates made from the indicated transfected cDNAs (squares for rat CaMKII and filled triangles for UNC-43) were tested for their ability to phosphorylate AC-2 in the presence of varying concentrations of calcium. The data were normalized to the maximal activity. (C) AC-2 kinase activities for S2 cell lysates from cells expressing the indicated cDNAs. White bars indicate the activity in the presence of calcium, whereas gray bars indicate the calcium-independent activity in the presence of EGTA. Error bars indicate the s.e.m. Significant differences in kinase activity were found $*P<0.05$ and $***P<0.001$ by one-way ANOVA followed by Bonferoni comparisons between the same transgenes (calcium versus EGTA). $n=3$ or more trials. (D) The calcium-independent activity (AC-2 kinase activity in the presence of EGTA, plotted as a percentage of the activity in the presence of calcium) of S2 lysates expressing the indicated form of UNC-43. Error bars indicate s.e.m. Significant differences in activity were observed $*P<0.05$ and $***P<0.001$, compared to levels in the WT group by one-way ANOVA followed by Bonferoni comparisons. $n=3$ or more trials.

independent CaMKII kinase activity (Yang and Schulman, 1999), and resulted in increased UNC-43::GFP neurite levels (Fig. 3J). The residues in this loop (H282 and R283) are thought to form electrostatic interactions with their partners in the catalytic domain (K148 and D238, respectively) (Yang and Schulman, 1999). Although mutations of K148 and D238 result in a calcium-independent CaMKII kinase activity (Yang and Schulman, 1999), surprisingly, these same mutations resulted in decreased UNC-43::GFP in neurites (Fig. 3J), which is the opposite phenotype from mutations in their salt bridge partners. These results suggest that although mutations that impair the interaction between the catalytic domain and the autoinhibitory domain result in calcium-independent CaMKII kinase activity, they do not automatically result in increased levels of UNC-43 in neurites. Thus, kinase activation itself does not stimulate UNC-43 neurite accumulation.

We next explored the idea that as yet unknown proteins might interact with UNC-43 by mimicking part of the autoinhibitory domain, thereby forming electrostatic interactions with some of the same residues on the catalytic domain. We generated an UNC-43(1-270)::GFP transgene that expresses a truncated UNC-43 containing only the catalytic domain. We found that UNC-43(1-270) accumulates to the same high levels observed for the α7 mutations (Fig. 3J). We also expressed the autoinhibitory domain and remaining C-terminal residues, called UNC-43(271-520), as a GFP chimera. UNC-43(271-520)::GFP does not accumulate to high levels in neurites (Fig. 3J). We also examined the electrostatic interactions between D238, which is in the catalytic domain, with R283E, which is in the autoinhibitory domain. D238R changes the side chain charge and results in a failure of UNC-43::GFP to accumulate in neurites (Fig. 3C,D). R283E replaces the side chain charge on the other side of this salt bridge, but results in the excessive neurite accumulation of UNC-43::GFP (Fig. 3E,F). We reasoned that a D238R R283E double mutant might partially restore the salt bridge, but would reverse the charge polarity in the bridge. When we introduced both of these mutations into UNC-43::GFP, we found that the mutant protein does not accumulate in neurites (Fig. 3G,H). Our results suggest that the D238R localization phenotype can mask the phenotype of R283E. We suggest that mutations in the autoinhibitory loop and the α7 helix, as well as in the hydrophobic regions of the catalytic domain with which α7 interacts, result in displacement of the autoinhibitory domain and exposure of regions on the catalytic domain required for translocation. Consistent with this idea, mutations in this key region of the catalytic domain can intragenically suppress mutations in the autoinhibitory domain.

Calcium-dependent kinase activity of UNC-43

We next wanted to confirm that UNC-43 has a similar calcium-dependent kinase activity as CaMKII. To test this possibility, we introduced an *unc-43* cDNA into an S2 expression vector, and transfected the resulting construct into S2 cells. For comparison to its vertebrate ortholog, we also transfected a plasmid containing the rat αCaMKII cDNA into S2 cells. We lysed the S2 cells and released similar amounts of UNC-43 and CaMKII protein as detected by western analysis against a C-terminal V5 epitope tag present on both proteins (Fig. 4A). Western blots of the lysates detected proteins of 54 kDa and 50 kDa for UNC-43 and CaMKII, respectively, indicating that the products produced by the insect cell lines were similar to the predicted sizes based on conceptual translation for each protein. To assay kinase activity, we incubated the proteins with autocamtide-2 (AC-2), a peptide substrate that contains the CaMKII R-X-X-S/T consensus phosphorylation site (Hanson et al., 1989). We incubated the kinase reactions either in EGTA or varying concentrations of calcium, and found that both UNC-43 and CaMKII calcium-dependent kinase activity was present (Fig. 4B and data not shown). We found that the kinase activity increased in response to increasing levels of free calcium, and that the maximum activity of both UNC-43 and CaMKII was observed at approximately 100 μM calcium. CaMKII and UNC-43 both displayed K_m values of ~20 μM for calcium, respectively. Lysates from mock-transfected S2 cells had low levels of kinase activity, and transfection of the UNC-43 and CaMKII cDNAs into S2 cells resulted in a ~20- to 100-fold increase in calcium-stimulated kinase activity in cell lysates.

To examine calcium-independent activity, we transfected either a wild-type UNC-43 cDNA or a cDNA containing the UNC-43(T286D) variant into S2 cells and obtained lysates. We tested the resulting UNC-43 proteins for kinase activity either in the presence or absence (using EGTA) of free calcium. For comparison, we also examined the calcium independence of rat αCaMKII and CaMKII(T286D). Rat CaMKII lysates contained kinase activity in the presence of calcium, and little activity in the absence (Fig. 4C). We measured the percentage calcium independence by comparing the ratio of the kinase activity in the absence of calcium relative to the amount of activity in the presence of calcium, and found that CaMKII from our S2 lysates showed ~1% calcium independence (Fig. 4C). By contrast, CaMKII(T286D) lysates contained similar levels of kinase activity in both the presence and absence of calcium. Robust kinase activity was present in UNC-43 lysates in the presence of calcium, and a small amount remained in its absence (Fig. 4C). The calcium independence of UNC-43 was ~5%, which was higher than the ~1% value observed for CaMKII. UNC-43(T286D) lysates contained similar levels of kinase activity in both the presence and absence of calcium. We also examined the calcium-independent kinase activity of our different mutant versions of UNC-43, and found that mutations reported to increase calcium-independent activity for CaMKII also increase calcium-independent activity for UNC-43 (Fig. 4D). Taken together, our results demonstrate that UNC-43 is a calcium-dependent kinase capable of phosphorylating CaMKII substrates. Like CaMKII, UNC-43 can be made into a calcium-independent form by mutating critical residues in either the catalytic or the autoinhibitory region.

In addition to mutations that were based on the CaMKI crystal structure (Goldberg et al., 1996),

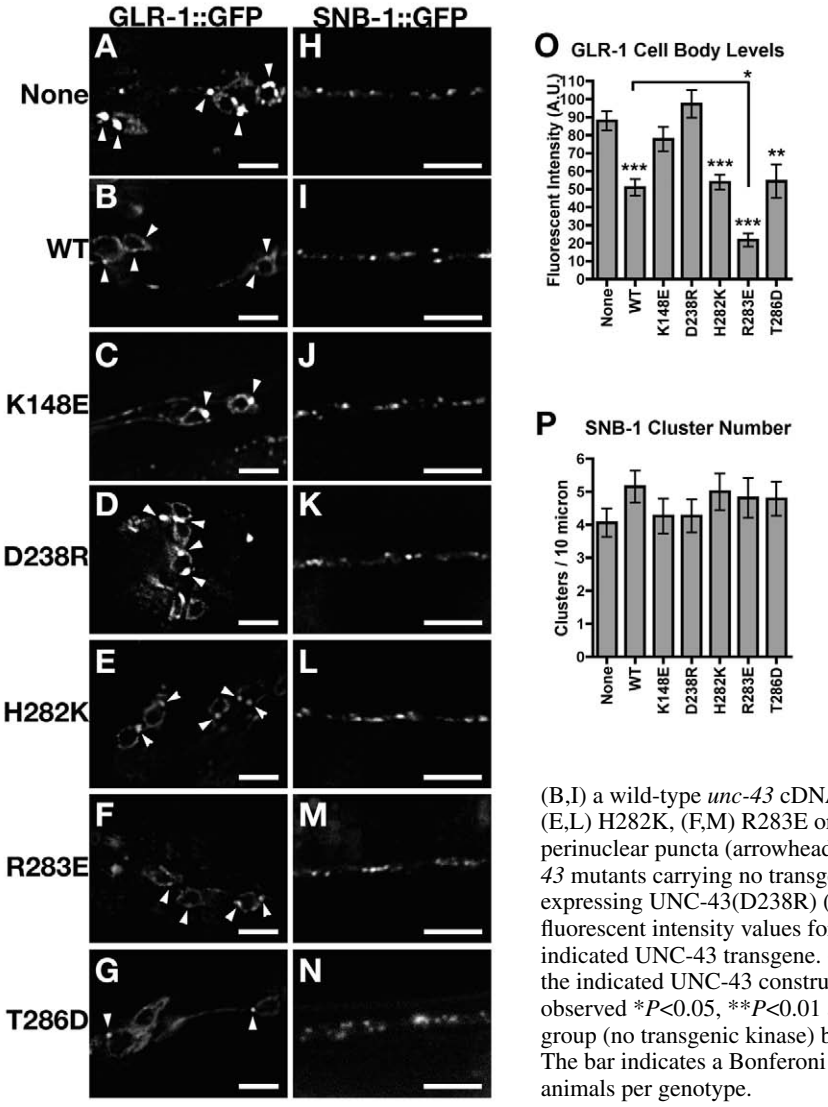

Fig. 5. UNC-43(K148E) and UNC-43(D238R) fail to rescue *unc-43* mutants for GLR-1 trafficking. (A-G) GLR-1::GFP in neurons cell bodies and (H-N) SNB-1::GFP in neurites were examined in *unc-43* mutants that also express either (A,H) no transgene, (B,I) a wild-type *unc-43* cDNA, or *unc-43* cDNA with the (C,J) K148E, (D,K) D238R, (E,L) H282K, (F,M) R283E or (G,N) T286D mutations. GLR-1::GFP is found in perinuclear puncta (arrowheads), and accumulates to high levels in these puncta in *unc-43* mutants carrying no transgene (A), or expressing UNC-43(K148E) (B) or expressing UNC-43(D238R) (C). (O) Fluorescence quantification measuring the mean fluorescent intensity values for neuronal cell bodies expressing GLR-1::GFP and the indicated UNC-43 transgene. (P) SNB-1::GFP cluster number in neurites expressing the indicated UNC-43 construct. Significant differences in fluorescence intensity were observed **P*<0.05, ***P*<0.01 and ****P*<0.001 when compared to levels in the 'None' group (no transgenic kinase) by one-way ANOVA followed by Bonferoni comparisons. The bar indicates a Bonferoni comparison between R283E and WT groups. *n*=10-30 animals per genotype.

there are mutations in UNC-43 that were identified in genetic screens based on the uncoordinated defects of *unc-43* mutants. A single gain-of-function mutant was identified, *unc-43(n498sd)*, which has semi-dominant phenotypes (paralyzed muscle contractions, defective egg laying and a decreased rate of defecation) that are opposite to those of the loss-of-function mutations (Reiner et al., 1999). Based on the genetic phenotype, we hypothesized that this mutation might cause constitutive and calcium-independent kinase activity. To test this, we introduced this mutation, E109K, into our UNC-43 S2 expression construct. Although we found that UNC-43(E109K) had reduced kinase activity and was less stable (data not shown), we also found that this change resulted in about 40% calcium-independent kinase activity (Fig. 4D). Interestingly, the E109K mutation, when introduced into UNC-43::GFP, showed no change in UNC-43::GFP translocation to the neurites (Fig. 3J). Our results suggest that the atonic behavioral defects observed in *unc-43(n498sd)* mutants are probably due to constitutive, calcium-independent activity of UNC-43.

UNC-43(K148E) and UNC-43(D238R) fail to rescue *unc-43* mutants for GLR-1 trafficking

As the K148E and D238R mutations affect the localization of UNC-43 within neurites, we reasoned that they might affect the ability of UNC-43 to regulate the trafficking of GLR-1. In *unc-43* loss-of-function mutants, GLR-1 accumulates to high levels in the cell body in perinuclear structures (Rongo and Kaplan, 1999). Expression of a wild-type *unc-43* cDNA in these same neurons using the *glr-1* promoter is sufficient to rescue *unc-43* mutants for this phenotype. To determine whether our mutations would impair UNC-43 function, we introduced the individual mutations into $P_{glr\text{-}1}$*::UNC-43*, the transgene we previously used to rescue *unc-43*. We introduced these individual transgenes into *unc-43* mutants that also express GLR-1::GFP, and we examined the cell body levels of GLR-1::GFP in the transgenic animals. As previously reported, *unc-43* mutants accumulated GLR-1::GFP in their cell bodies (Rongo and Kaplan, 1999) (Fig. 5A), and this defect was corrected in animals that also expressed a wild-type *unc-43* cDNA (Fig. 5B). Mutants expressing UNC-43(K148E) or UNC-43(D238R) accumulated high levels of punctate GLR-1::GFP in their cell body, indicating that the mutant proteins failed to rescue these *unc-43* mutants (Fig. 5C,D,O). Mutants expressing UNC-43 with either the H282K or T286D mutations had wild-type levels of GLR-1::GFP in their cell bodies, indicating that the mutant proteins rescued *unc-43* (Fig. 5E,G,O). Mutants expressing UNC-43(R283E) had a small but significant decrease in GLR-1::GFP cell bodies levels compared to the wild type (Fig. 5F,O). These results demonstrate that mutations in the catalytic domain that decrease UNC-43 localization to neurites also decrease UNC-43 function with respect to GLR-1 trafficking, whereas mutations in the autoinhibitory domain that increase UNC-43 localization to neurites do not diminish UNC-43 function.

As the mutations in the catalytic domain impaired UNC-43 function and neurite localization, we also examined whether they might result in more general defects in synapse formation. We introduced $P_{glr\text{-}1}$*::UNC-43* and its mutant variants into nematodes that also express a synaptobrevin-GFP reporter, SNB-1::GFP, previously used to label synapses to GLR-1-expressing interneurons (Jorgensen and Nonet, 1995; Rongo et al., 1998). For both wild-type and mutant transgenes, we observed no defects in general development, morphology, axon guidance or neurite outgrowth (data not shown). In all cases we observed normal SNB-1:GFP levels and normal numbers of SNB-1::GFP-labeled presynaptic boutons (Fig. 5H-N,P). Thus, our results suggest that our mutant transgenes do not affect more obvious aspects of these neurons.

The voltage-dependent calcium channel UNC-2 is required for UNC-43 translocation

As UNC-43 is a calcium-dependent kinase, we reasoned that the opening of a calcium channel results in the activation and subsequent translocation of UNC-43. The *unc-2* gene encodes an α subunit of a voltage-dependent calcium channel and *unc-2* loss-of-function mutations have a similar phenotype to *unc-43* loss-of-function mutations (Rongo and Kaplan, 1999; Schafer and Kenyon, 1995). To test whether UNC-2 is also required for UNC-43 translocation, we introduced UNC-43::GFP into *unc-2* loss-of-function mutants to observe its localization. Both wild-type and *unc-2* mutant nematodes

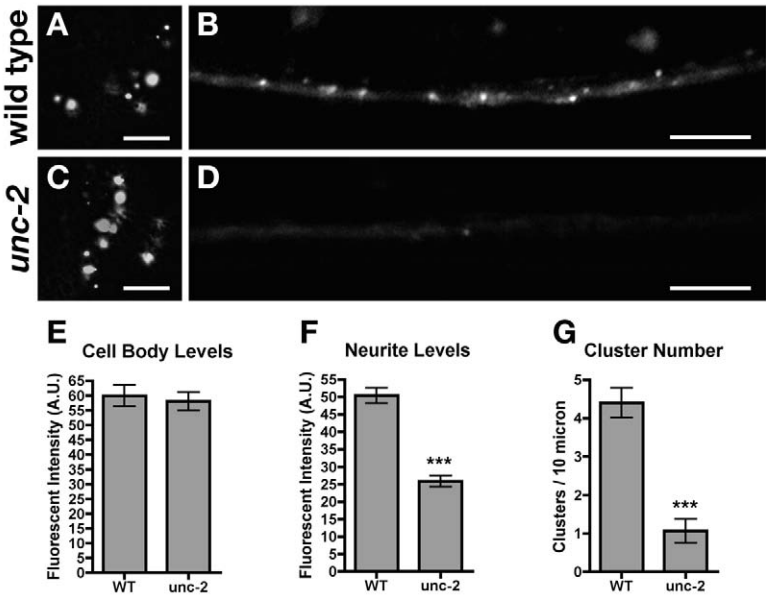

Fig. 6. UNC-2 regulates UNC-43 abundance in neurites. (A,C) Cell bodies and (B,D) neurites expressing wild-type UNC-43::GFP in (A,B) wild-type animals, or (C,D) in *unc-2(e55)* animals. Mutations in *unc-2* result in the failure of UNC-43 to accumulate throughout the unlocalized neurite pool (D). Fluorescence quantification measuring the mean fluorescent intensity values for (E) neuron cell bodies and (F) neurites expressing UNC-43::GFP in either wild-type (WT) or *unc-2(e55)* mutant animals. (G) The number of clusters (clusters defined as above a threshold of two standard deviation values of the mean outside of the clustered signal) per 10 μm length of neurite for the indicated genotypes. A.U., arbitrary units. Error bars indicate s.e.m. Highly significant differences (***P<0.0001) in cluster number and neurite levels were observed in *unc-2* mutants compared to levels in the WT control group using the Student's t-test. n=8 animals for each genotype. Bar, 5 μm.

contained similar levels of cellular UNC-43::GFP (Fig. 6A,C,E). However, although wild-type nematodes contained abundant UNC-43::GFP in their neurites (Fig. 6B), *unc-2* mutants contained low neurite levels of the kinase (Fig. 6F). Interestingly, *unc-2* loss-of-function mutants also contained fewer clusters of UNC-43::GFP (Fig. 6G). Taken together, our results suggest that UNC-2 regulates two different aspects of UNC-43 neurite localization: the amount of UNC-43 that accumulates in the unlocalized neurite pool and the amount of UNC-43 that accumulates in clusters.

Discussion

In an attempt to understand UNC-43 function and localization, we found that a GFP-tagged UNC-43 protein, when expressed in *C. elegans* neurons, is localized both in clusters and in a diffuse pool throughout neurites. We examined the effect on both kinase activity and subcellular localization of several mutations in amino acids thought to mediate interactions between the catalytic domain and the autoinhibitory domain. The majority of mutations that disrupt these interactions result in increased calcium-independent activity, and most also result in the increased amount of UNC-43 present in the neurites. To our surprise, we identified two residues in the catalytic core (K148 and D238) that do not impair kinase activity but nevertheless are important for UNC-43 localization and function in neurites. Moreover, we have shown that the activity of UNC-2, a voltage-dependent calcium channel, is also required to localize UNC-43 to neurites.

Vertebrate CaMKII has previously been shown to be localized to dendrites and enriched at the PSD (Ouimet et al., 1984; Petersen et al., 2003; Strack et al., 1997). In addition, CaMKII can form non-synaptic clusters, with increasing amounts of these clusters forming in response to ischemic stress (Tao-Cheng et al., 2002). We find that UNC-43 forms clusters both in neurites and in the neuron cell bodies.

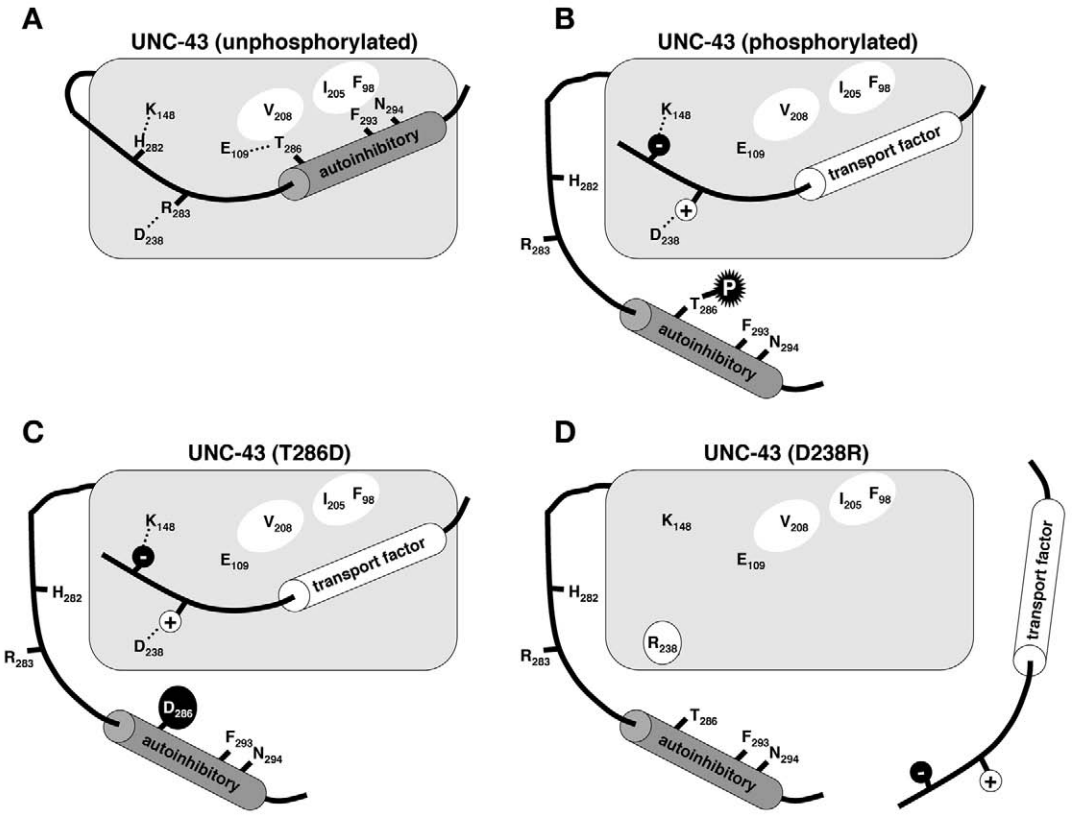

Fig. 7. Model for the amino acid interactions that regulate UNC-43 localization. A schematic model for UNC-43 regulatory amino acid interactions between the catalytic domain (the gray box) and the autoinhibitory domain (the black line and gray cylinder). Electrostatic interactions between amino acid side chains are indicated by a dotted line. Hydrophobic pockets created within the catalytic domain are indicated by the white ovals. A hypothetical factor that transports UNC-43 to the neurites is indicated by the white cylinder. Negatively-charged side chains are indicated by black circles, whereas positively-charged side chains are indicated by white circles. The black star in B indicates the addition of a phosphate at T286. (A) In the absence of activity, UNC-43 is kept quiescent by amino acid interactions between the catalytic domain and the autoinhibitory domain. (B) Upon calcium activation, calmodulin (not shown) binds and displaces the autoinhibitory domain, allowing for autophosphorylation at T286. The residues K148 and D238 are made available to bind to outside factors that facilitate the translocation of UNC-43 to neurites. (C) The T286D mutation mimics phosphorylation, even in the absence of calcium stimulation, by introducing charge at T286, displacing the autoinhibitory domain from the hydrophobic pocket along the catalytic domain. This constitutively exposes K148 and D238 for binding to outside factors, resulting in the over-transport of UNC-43 to the neurites. (D) The D238R mutation destabilizes an electrostatic interaction required for the autoinhibitory domain to bind to the catalytic domain, thereby resulting in constitutive kinase activity. The mutation also destabilizes a separate electrostatic interaction required for the catalytic domain to interact with the transport factors that facilitate UNC-43 localization to the neurites.

Interestingly, the clusters found in the cell bodies colocalize with clusters of GLR-1 found at the Golgi. UNC-43 activity is required for the transport of GLR-1 from the cell body to the synaptic connections of the neurites, and UNC-43 kinase activity is required for this function (Rongo and Kaplan, 1999). Thus, the colocalization of UNC-43 with GLR-1 at or near the Golgi would suggest that UNC-43 is phosphorylating target molecules that participate in the secretory trafficking of GLR-1, perhaps at these initial regions of protein translocation. UNC-43 is also found to colocalize with GLR-1 along neurites, although a large fraction of UNC-43 clusters do not colocalize. It is possible that this latter population of UNC-43 clusters are at non-glutamatergic synaptic inputs; alternatively, they might be non-synaptic accumulations of UNC-43. There is also an abundant, unlocalized pool of UNC-43 present throughout the neurites. This unlocalized pool of UNC-43 could be functionally important for synapses even though it is not directly at the PSD. For example, the insertion of new glutamate receptors in response to activity is thought to occur by mobilizing receptors from a subsynaptic pool present beneath the PSD and along the length of the dendrites (for reviews, see Malenka, 2003; Malinow, 2003; Sheng and Hyoung Lee, 2003; Song and Huganir, 2002). Recently, the endocytosis of glutamate receptors has been shown to occur at specialized regions outside of the PSD (Racz et al., 2004). Thus, it is reasonable that UNC-43 could be regulating PSD composition and/or function with its presence in an unlocalized pool in the neurites. Consistent with this idea, two mutations in *unc-43* (K148E and D238R) that diminish UNC-43 levels in the unlocalized neurite pool also prevent UNC-43 from regulating GLR-1 localization.

Our findings also demonstrate that the UNC-2 voltage-dependent calcium channel is required for UNC-43 to accumulate in neurites, thereby providing a means for neural activity to regulate the localization of UNC-43. Activity has been shown to have an important role in CaMKII translocation in neurons (Leonard et al., 1999; Ouyang et al., 1997; Shen and Meyer, 1999; Shen et al., 2000; Strack et al., 1997). For example, activated NMDA receptors can mobilize αCaMKII within neurons to dendrites (Bayer et al., 2001; Shen and Meyer, 1999; Shen et al., 2000). In addition, activated CaMKII can become trapped at PSDs, and this form of localization trapping could mark active synapses and place CaMKII near a source of calcium influx (Shen et al., 2000). In *unc-43* gain-of-function mutants like T286D and R283E that mimic increased neuronal activity, we observed an increase of UNC-43 in neurites, but did not observe an increase at PSDs. In *unc-2* mutants, where neuronal activity is decreased, we observed both a decrease of UNC-43 in neurites and a decrease of UNC-43 at PSDs. We speculate that activity regulates CaMKII localization through two steps, neurite translocation and PSD trapping, and that at least the former step has been conserved evolutionarily in *C. elegans* interneurons.

Our mutational analysis of UNC-43 suggests a possible mechanism by which the translocation of the kinase might occur in response to calcium (Fig. 7). Calcium/calmodulin binding to the autoinhibitory domain can cause the domain to become displaced from the hydrophobic pocket on the catalytic domain to which it binds. Transport factors that are similar in sequence to the autoinhibitory domain could then insert themselves along this same hydrophobic pocket, thus physically tethering the kinase to such factors as they make their way out to the neurites. In such a scenario, the autoinhibitory domain would be competing against these hypothetical transport factors for access to the catalytic domain; hence, mutations that impair the ability of the autoinhibitory domain to interact with the catalytic domain should result in increased amounts of UNC-43 in the neurites. This was indeed the case for most of the mutations we examined, including a deletion mutant that results in the complete removal of the autoinhibitory domain. Only mutations in key residues of the catalytic domain that not only interacted with the autoinhibitory domain but also the transport factor would be expected to have the opposite phenotype, thus decreasing the amount of UNC-43 in the neurites. We found two such mutations, D238 and K148, suggesting that these residues have an important role in the translocation of UNC-43 to the neurites.

What is the nature of the transport factor? One protein thought to bind to αCaMKII by mimicking the pseudosubstrate domain is the NR2B subunit of the NMDA receptor, which contains a short sequence in its C-terminal tail that matches the CaMKII consensus site (Bayer et al., 2001). The *C. elegans* ortholog of NR2 lacks this same sequence, however, and NMDA receptor knockout mutants have little effect on UNC-43 localization (Brockie et al., 2001) (data not shown). The UNC-2 α1 calcium channel subunit is required for UNC-43 localization, but also lacks the CaMKII consensus site (Mathews et al., 2003). CaMKII probably associates with other proteins for its trafficking, in addition to NR2B. Thus, it is reasonable to expect that some of these proteins will be common interactors for both CaMKII and UNC-43.

We thank A. Fire, A. Fraser (Sanger Institute), R. Herman (CGC), J. Kaplan, M. Kennedy, Y. Kohara, V. Maricq, J. Mendel, C. Mello, M. Nonet, H. Schulman, T. Stiernagle (CGC) and R. Tsien for reagents and strains. We thank Bonnie Firestein for critical comments on the manuscript. C.R. is a Pew Scholar in the Biomedical Sciences. Additional funding was provided by the N.I.H. (R01 NS42023) and a Grant-In-Aid from the American Heart Association.

References

Bayer, K. U., De Koninck, P., Leonard, A. S., Hell, J. W. and Schulman, H. (2001). Interaction with the NMDA receptor locks CaMKII in an active conformation. *Nature* **411**, 801-805.

Brocke, L., Chiang, L. W., Wagner, P. D. and Schulman, H. (1999). Functional implications of the subunit composition of neuronal CaM kinase II. *J. Biol. Chem.* **274**, 22713-22722.

Brockie, P. J., Madsen, D. M., Zheng, Y., Mellem, J. and Maricq, A. V. (2001). Differential expression of glutamate receptor subunits in the nervous system of Caenorhabditis elegans and their regulation by the homeodomain protein UNC-42. *J. Neurosci.* **21**, 1510-1522.

Chalfie, M., Sulston, J. E., White, J. G., Southgate, E., Thomson, J. N. and Brenner, S. (1985). The neural circuit for touch sensitivity in *C. elegans*. *J. Neurosci.* **5**, 956-964.

Chen, N., Harris, T. W., Antoshechkin, I., Bastiani, C., Bieri, T., Blasiar, D., Bradnam, K., Canaran, P., Chan, J., Chen, C. K. et al. (2005). WormBase: a comprehensive data resource for *Caenorhabditis* biology and genomics. *Nucleic Acids Res* **33** (Database Issue), D383-D389.

Firestein, B. L. and Rongo, C. (2001). DLG-1 is a MAGUK similar to SAP97 and is required for adherens junction formation. *Mol. Biol. Cell* **12**, 3465-3475.

Fong, Y. L., Taylor, W. L., Means, A. R. and Soderling, T. R. (1989). Studies of the regulatory mechanism of Ca2+/calmodulin-dependent protein kinase

II. Mutation of threonine 286 to alanine and aspartate. *J. Biol. Chem.* **264**, 16759-16763.

Gaertner, T. R., Kolodziej, S. J., Wang, D., Kobayashi, R., Koomen, J. M., Stoops, J. K. and Waxham, M. N. (2004). Comparative analyses of the three-dimensional structures and enzymatic properties of alpha, beta, gamma and delta isoforms of Ca2+-calmodulin-dependent protein kinase II. *J. Biol. Chem.* **279**, 12484-12494.

Glodowski, D. R., Wright, T., Martinowich, K., Chang, H. C., Beach, D. and Rongo, C. (2005). Distinct LIN-10 domains are required for its neuronal function, its epithelial function, and its synaptic localization. *Mol. Biol. Cell* **16**, 1417-1426.

Goldberg, J., Nairn, A. C. and Kuriyan, J. (1996). Structural basis for the autoinhibition of calcium/calmodulin-dependent protein kinase I. *Cell* **84**, 875-887.

Hanson, P. I., Kapiloff, M. S., Lou, L. L., Rosenfeld, M. G. and Schulman, H. (1989). Expression of a multifunctional Ca2+/calmodulin-dependent protein kinase and mutational analysis of its autoregulation. *Neuron* **3**, 59-70.

Hanson, P. I., Meyer, T., Stryer, L. and Schulman, H. (1994). Dual role of calmodulin in autophosphorylation of multifunctional CaM kinase may underlie decoding of calcium signals. *Neuron* **12**, 943-956.

Hart, A. C., Sims, S. and Kaplan, J. M. (1995). Synaptic code for sensory modalities revealed by *C. elegans* GLR-1 glutamate receptor. *Nature* **378**, 82-84.

Hayashi, Y., Shi, S. H., Esteban, J. A., Piccini, A., Poncer, J. C. and Malinow, R. (2000). Driving AMPA receptors into synapses by LTP and CaMKII: requirement for GluR1 and PDZ domain interaction. *Science* **287**, 2262-2267.

Hinds, H. L., Tonegawa, S. and Malinow, R. (1998). CA1 long-term potentiation is diminished but present in hippocampal slices from alpha-CaMKII mutant mice. *Learn. Mem.* **5**, 344-354.

Hoelz, A., Nairn, A. C. and Kuriyan, J. (2003). Crystal structure of a tetradecameric assembly of the association domain of Ca2+/calmodulin-dependent kinase II. *Mol. Cell* **11**, 1241-1251.

Hudmon, A. and Schulman, H. (2002). Neuronal CA2+/calmodulin-dependent protein kinase II: the role of structure and autoregulation in cellular function. *Annu. Rev. Biochem.* **71**, 473-510.

Ito, I., Hidaka, H. and Sugiyama, H. (1991). Effects of KN-62, a specific inhibitor of calcium/calmodulin-dependent protein kinase II, on long-term potentiation in the rat hippocampus. *Neurosci. Lett.* **121**, 119-121.

Jorgensen, E. M. and Nonet, M. L. (1995). Neuromuscular junctions in the nematode *C. elegans*. *Sem. Dev. Biol.* **6**, 207-220.

Leonard, A. S., Lim, I. A., Hemsworth, D. E., Horne, M. C. and Hell, J. W. (1999). Calcium/calmodulin-dependent protein kinase II is associated with the N-methyl-D-aspartate receptor. *Proc. Natl. Acad. Sci. USA* **96**, 3239-3244.

Lisman, J. E. and Goldring, M. A. (1988). Feasibility of long-term storage of graded information by the Ca2+/calmodulin-dependent protein kinase molecules of the postsynaptic density. *Proc. Natl. Acad. Sci. USA* **85**, 5320-5324.

Malenka, R. C. (2003). Synaptic plasticity and AMPA receptor trafficking. *Ann. New York Acad. Sci.* **1003**, 1-11.

Malenka, R. C., Kauer, J. A., Perkel, D. J., Mauk, M. D., Kelly, P. T., Nicoll, R. A. and Waxham, M. N. (1989). An essential role for postsynaptic calmodulin and protein kinase activity in long-term potentiation. *Nature* **340**, 554-557.

Malinow, R. (2003). AMPA receptor trafficking and long-term potentiation. *Philos. Trans. R. Soc. London Ser. B* **358**, 707-714.

Malinow, R., Schulman, H. and Tsien, R. W. (1989). Inhibition of postsynaptic PKC or CaMKII blocks induction but not expression of LTP. *Science* **245**, 862-866.

Maricq, A. V., Peckol, E., Driscoll, M. and Bargmann, C. I. (1995). Mechanosensory signalling in *C. elegans* mediated by the GLR-1 glutamate receptor. *Nature* **378**, 78-81.

Mathews, E. A., Garcia, E., Santi, C. M., Mullen, G. P., Thacker, C., Moerman, D. G. and Snutch, T. P. (2003). Critical residues of the Caenorhabditis elegans unc-2 voltage-gated calcium channel that affect behavioral and physiological properties. *J. Neurosci.* **23**, 6537-6545.

Meador, W. E., Means, A. R. and Quiocho, F. A. (1993). Modulation of calmodulin plasticity in molecular recognition on the basis of x-ray structures. *Science* **262**, 1718-1721.

Mukherji, S. and Soderling, T. R. (1994). Regulation of Ca2+/calmodulin-dependent protein kinase II by inter- and intrasubunit-catalyzed autophosphorylations. *J. Biol. Chem.* **269**, 13744-13747.

Mukherji, S., Brickey, D. A. and Soderling, T. R. (1994). Mutational analysis of secondary structure in the autoinhibitory and autophosphorylation domains of calmodulin kinase II. *J. Biol. Chem.* **269**, 20733-20738.

Ouimet, C. C., McGuinness, T. L. and Greengard, P. (1984). Immunocytochemical localization of calcium/calmodulin-dependent protein kinase II in rat brain. *Proc. Natl. Acad. Sci. USA* **81**, 5604-5608.

Ouyang, Y., Kantor, D., Harris, K. M., Schuman, E. M. and Kennedy, M. B. (1997). Visualization of the distribution of autophosphorylated calcium/calmodulin-dependent protein kinase II after tetanic stimulation in the CA1 area of the hippocampus. *J. Neurosci.* **17**, 5416-5427.

Petersen, J. D., Chen, X., Vinade, L., Dosemeci, A., Lisman, J. E. and Reese, T. S. (2003). Distribution of postsynaptic density (PSD)-95 and Ca2+/calmodulin-dependent protein kinase II at the PSD. *J. Neurosci.* **23**, 11270-11278.

Racz, B., Blanpied, T. A., Ehlers, M. D. and Weinberg, R. J. (2004). Lateral organization of endocytic machinery in dendritic spines. *Nat. Neurosci.* **7**, 917-918.

Reiner, D. J., Newton, E. M., Tian, H. and Thomas, J. H. (1999). Regulation of a behavioral clock, muscle excitation, and two genetically defined targets by the *C. elegans unc-43* CaM Kinase II. *Nature* **402**, 199-203.

Rich, R. C. and Schulman, H. (1998). Substrate-directed function of calmodulin in autophosphorylation of Ca2+/calmodulin-dependent protein kinase II. *J. Biol. Chem.* **273**, 28424-28429.

Rongo, C. (2002). A fresh look at the role of CaMKII in hippocampal synaptic plasticity and memory. *BioEssays* **24**, 223-233.

Rongo, C. and Kaplan, J. K. (1999). CaMKII regulates the density of central glutamatergic synapses in vivo. *Nature* **402**, 195-199.

Rongo, C., Whitfield, C. W., Rodal, A., Kim, S. K. and Kaplan, J. M. (1998). LIN-10 is a shared component of the polarized protein localization pathways in neurons and epithelia. *Cell* **94**, 751-759.

Schafer, W. R. and Kenyon, C. J. (1995). A calcium-channel homologue required for adaptation to dopamine and serotonin in Caenorhabditis elegans. *Nature* **375**, 73-78.

Shen, K. and Meyer, T. (1999). Dynamic control of CaMKII translocation and localization in hippocampal neurons by NMDA receptor stimulation. *Science* **284**, 162-166.

Shen, K., Teruel, M., Connor, J., Shenolikar, S. and Meyer, T. (2000). Molecular memory by reversible translocation of calcium/calmodulin-dependent protein kinase II. *Nat. Neurosci.* **3**, 881-886.

Sheng, M. and Hyoung Lee, S. (2003). AMPA receptor trafficking and synaptic plasticity: major unanswered questions. *Neurosci. Res.* **46**, 127-134.

Shim, J., Umemura, T., Nothstein, E. and Rongo, C. (2004). The unfolded protein response regulates glutamate receptor export from the endoplasmic reticulum. *Mol. Biol. Cell* **15**, 4818-4828.

Silva, A. J., Paylor, R., Wehner, J. M. and Tonegawa, S. (1992a). Impaired spatial learning in alpha-calcium-calmodulin kinase II mutant mice. *Science* **257**, 206-211.

Silva, A. J., Stevens, C. F., Tonegawa, S. and Wang, Y. (1992b). Deficient hippocampal long-term potentiation in alpha-calcium-calmodulin kinase II mutant mice. *Science* **257**, 201-206.

Song, I. and Huganir, R. L. (2002). Regulation of AMPA receptors during synaptic plasticity. *Trends Neurosci.* **25**, 578-588.

Strack, S., Choi, S., Lovinger, D. M. and Colbran, R. J. (1997). Translocation of autophosphorylated calcium/calmodulin-dependent protein kinase II to the postsynaptic density. *J. Biol. Chem.* **272**, 13467-13470.

Tao-Cheng, J. H., Vinade, L., Pozzo-Miller, L. D., Reese, T. S. and Dosemeci, A. (2002). Calcium/calmodulin-dependent protein kinase II clusters in adult rat hippocampal slices. *Neuroscience* **115**, 435-440.

Waldmann, R., Hanson, P. I. and Schulman, H. (1990). Multifunctional Ca2+/calmodulin-dependent protein kinase made Ca2+ independent for functional studies. *Biochemistry* **29**, 1679-1684.

White, J. G., Southgate, E., Thomson, J. N. and Brenner, S. (1986). The structure of the nervous system of *C. elegans*. *Philos. Trans. R. Soc. London Ser. B* **314**, 1-340.

Wood, W. B. (1988). *The Nematode c. Elegans*. Cold Spring Harbor: Cold Spring Harbor Laboratory.

Yang, E. and Schulman, H. (1999). Structural examination of autoregulation of multifunctional calcium/calmodulin-dependent protein kinase II. *J. Biol. Chem.* **274**, 26199-26208.